INTERNATIONAL JOURNAL OF NUMERICAL MODELLING: ELECTRONIC NETWORKS, DEVICES AND FIELDS
Int. J. Numer. Model. 2014; **27**:79–88
Published online 6 May 2013 in Wiley Online Library (wileyonlinelibrary.com). DOI: 10.1002/jnm.1895

A simple and accurate dynamical modeling of quantum-dot semiconductor optical amplifiers

Hussein Taleb[1], Kambiz Abedi[1,*] and Saeed. Golmohammadi[2]

[1]*Department of Electrical Engineering, Faculty of Electrical and Computer Engineering, Shahid Beheshti University, G. C. 18993443332 Tehran, Iran*
[2]*Nanophotonics Group, School of Engineering-Emerging Technologies, University of Tabriz, Tabriz 5166614761, Iran*

SUMMARY

In this article, quantum-dot semiconductor optical amplifiers (QD-SOAs) have been modelled using state space method. To derive this model, we have manipulated the rate equation model of the QD-SOA, where the average values of the occupation probabilities along the QD-SOA cavity are considered as the state variables of the system. Using these variables, the distance dependence of the rate equations is eliminated. The derived state space model gives the optical gain and output signal of the amplifier with a high accuracy. Simulation results show that the derived model is not only much simpler and faster than conventional rate equation models, but also the optical gain and output signal of the investigated QD-SOA are calculated with a higher precision compared to the rate equation model. Copyright © 2013 John Wiley & Sons, Ltd.

Received 18 March 2012; Accepted 14 February 2013

KEY WORDS: quantum-dot; rate equation model; semiconductor optical amplifiers; state space model

1. INTRODUCTION

Quantum-dot semiconductor optical amplifiers (QD-SOAs) have been intensively investigated during the last decade. Both theoretical and experimental studies have proven the unique capabilities of these devices. Ultrafast gain recovery [1–5], high saturated output power [6, 7], pattern-effect free signal amplification at high speeds up to 80 Gb/s [8–10], pattern-effect free XGM-based wavelength conversion at 160 Gb/s [11], capability of operation at terabits per second speeds in presence of a control signal [12], amplification of high bit rate multichannel signals [13, 14], low noise figure [15], small dimensions, and integration with other optoelectronic devices such as laser diodes and modulators are the main advantages of QD-SOAs.

In recent years, several models have been proposed for the description of the electrical and optical characteristics of QD-SOAs. Among these theoretical models, the most accurate models are based on semiconductor Maxwell–Bloch equations [16–20]. However, the numerical calculations associated with this model are extremely time-consuming and requires huge amount of memory. A simplified approach to model QD-SOAs which is known as rate equation model (REM), has demonstrated an excellent agreement with experimental results [4, 21]. The REM includes a set of coupled differential equations to give details of carrier dynamics and optical properties of QD-SOA. To include the carrier dynamics in the REM, in some papers, the electron–hole pairs are considered as exciton and only the carrier dynamics in the conduction band is taken into account [22–25]. In some other papers, the holes dynamics is included by using quasi-Fermi level in the valence band (VB) [26]. Also, the dynamics of electron and hole are considered separately in some articles [27–31] and [4]. This model is known as 'electron–hole model' [30],

*Correspondence to: Kambiz Abedi, Department of Electrical Engineering, Faculty of Electrical and Computer Engineering, Shahid Beheshti University, G. C. 18993443332, Tehran, Iran
E-mail: k_abedi@sbu.ac.ir

where the rate equations for electrons and holes are written separately. In this paper, we have employed the last approach to give details of the investigated QD-SOA [29, 31].

Although the REM of QD-SOA is much simpler and faster than QD Maxwell–Bloch equations, because of time as well as distance dependence of the rate equations, the long computation time is still a big concern in some applications. Furthermore, because the simulation run time is very sensitive to the distance between two adjacent nodes in the spaced distance-time grid, a huge memory may be required during the simulation execution, especially in condition that a long sequence of optical pulses have to be considered in numerical simulations. Therefore, our objective in this paper is to derive a simple and efficient dynamical model for QD-SOA that calculates the optical gain and output of the device with an acceptable precision. For this purpose, the average values of occupation probabilities along the QD-SOA cavity are considered as the variables of the system and the distance dependence of the REM is eliminated. In the state space model (SSM), the QD-SOA is considered as a black box, that is, it is viewed mainly in terms of its input and output characteristics.

This paper is organized as follows. In Section 2, the physical structure of the investigated QD-SOA as well as the rate equations of the device are presented. In Section 3, we derive an SSM for QD-SOA. Comparison between the results obtained from SSM with results of the REM is presented in Section 4. Finally, Section 5 gives a summary of our work.

2. PHYSICAL MODEL AND THEORY

The investigated device is an InAs/GaAs QD-SOA that operates around 1.3 μm. A tenfold stacked QD active region is sandwiched between two AlGaAs cladding layers. The self-assembled InAs QDs in each layer are covered with a 5-nm-thick InGaAs capping layer. The QD layers are separated by 33-nm-thick p-doped GaAs spacer layers. The physical structure of our investigated QD-SOA is illustrated in Fig. 1. The state space model of the QD-SOA is based on rate equation model which was given in [16]. The essence of the state space model of the QD-SOA can be summarized as follows. First, it is considered that self-assembled QDs have a size distribution with a Gaussian profile and consist of 181 spectral groups. In each QD group, it is assumed that all QDs are identical. The separation between the transition energies of two adjacent groups is assumed to be $\Delta E = 1$ meV. Second, it is assumed that all QDs are spatially isolated and therefore each QD can exchange only with a common carrier reservoir. It is assumed that the quantum well (QW) and wetting layer (WL) states are degenerate. Therefore a many-fold degenerate energy state is considered in the band diagram to model the effect of the carrier reservoir. Third, the homogeneous broadening of QD transitions is described by a Lorentzian function. The energy band diagram of the *j*-th QD spectral group is shown in Fig. 2. As an example, the relative energy positions of the most probable QD group are designated in the figure [12]. As can be seen in the figure, each QD group has three energy

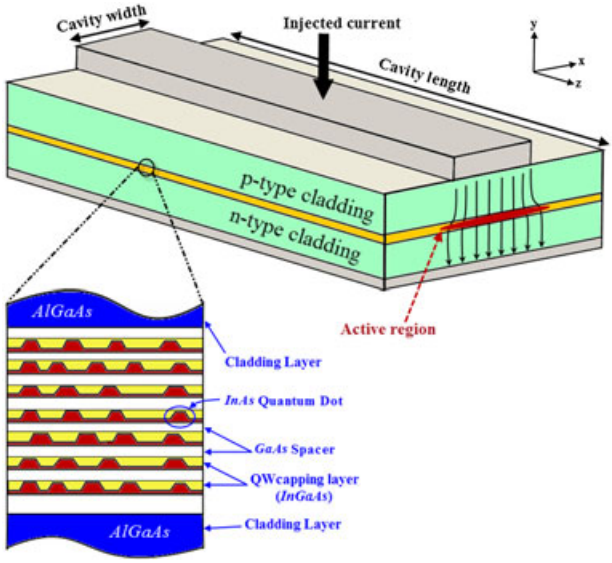

Figure 1. The physical structure of a travelling-wave QD-SOA.

DOI: 10.1002/jnm

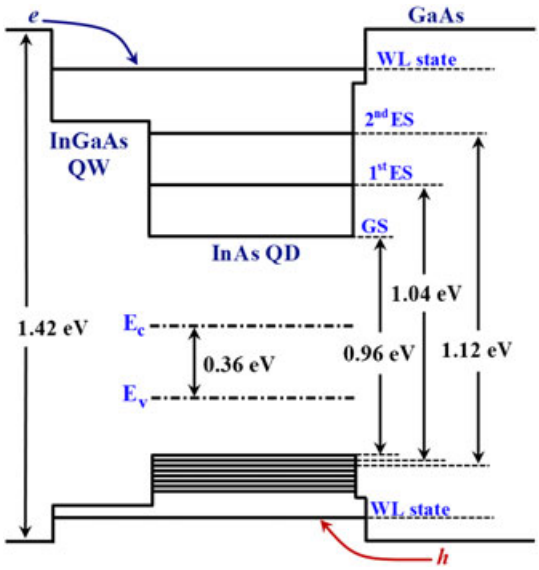

Figure 2. The energy band diagram of the active region of the quantum-dot semiconductor optical amplifier (QD-SOA). The energy separations of the QD electron and hole states are 70 and 10 meV, respectively. The radiative transitions are shown in the figure.

levels in the conduction band (CB) and three energy levels in the valence band (VB). The self-assembled QDs have three non-degenerate energy levels in the conduction band and eight non-degenerate energy levels in the VB and are accompanied by two dimensional wetting layer (WL) states [29].

The dynamic behavior of the QD-SOA is determined by photon as well as carrier rate equations. Details of the REM of the investigated QD-SOA can be found in [29, 31] and are summarized as follows:
Photon rate equation

$$\frac{\partial S}{\partial z} = g_{QD}S - \alpha S \tag{1}$$

where

$$g_{QD} = \sum_{j=0}^{H} g_j\left(f_j^n + f_j^p - 1\right) \tag{2}$$

where

$$g_j = g_j^{\max}\frac{\hbar\omega_j^{\max}}{\hbar\omega}\exp\left(\frac{-\left(\hbar\omega - \hbar\omega_j^{\max}\right)^2}{2\sigma_j^2}\right) \tag{3}$$

i. Electron states rate equations.

For the GS,

$$\frac{\partial f_0^n}{\partial t} = \left(R_{1,0}^{nc} - R_{0,1}^{ne}\right) - R_0^{sp} - R_0^{st} \tag{4}$$

For the ith ES ($i = 1, 2$),

$$\frac{\partial f_i^n}{\partial t} = \left(R_{i+1,i}^{nc} - R_{i,i+1}^{ne}\right) - \left(R_{i,i-1}^{nc} - R_{i-1,i}^{ne}\right) - R_i^{sp} - R_i^{st}. \tag{5}$$

For the WL state,

$$\frac{\partial w_n}{\partial t} = \frac{I}{qV_aN_{WL}} - \left(R_{w_n,2}^{nc} - R_{2,w_n}^{ne}\right) - R_{w_n}^{sp} \tag{6}$$

DOI: 10.1002/jnm

where

$$R_{i+1,i}^{nc} = \frac{\left(1-f_i^n\right)f_{i+1}^n}{\tau_{i+1,i}^n}\left(a_{i+1,i}^n + c_{i+1,i}^{np}w_p + c_{i+1,i}^{nn}w_n\right) \tag{7}$$

$$R_{i,i+1}^{ne} = \frac{f_i^n\left(1-f_{i+1}^n\right)}{\tau_{i,i+1}^n}\left(a_{i,i+1}^n + c_{i,i+1}^{np}w_p + c_{i,i+1}^{nn}w_n\right) \tag{8}$$

$$R_i^{sp} = \frac{f_i^n f_i^p}{\tau_{iR}}\left(a_{ii}^n + c_{ii}^p f_i^p + c_{ii}^n f_i^n\right) \tag{9}$$

$$R_i^{st} = \frac{v_g g_i}{N_Q}\left(f_i^p + f_i^n - 1\right)S \tag{10}$$

ii. Hole states rate equations.

For the GS,

$$\frac{\partial f_0^p(t)}{\partial t} = \left(R_{1,0}^{pc} - R_{0,1}^{pe}\right) - R_0^{sp} - R_0^{st} \tag{11}$$

For the kth ES ($k = 1, 2$),

$$\frac{\partial f_k^p(t)}{\partial t} = \left(R_{k+1,k}^{pc} - R_{k,k+1}^{pe}\right) - \left(R_{k,k-1}^{pc} - R_{k-1,k}^{pe}\right) - R_k^{sp} - R_k^{st} \tag{12}$$

For the kth ES ($3 \le k \le 7$),

$$\frac{\partial f_k^p}{\partial t} = \left(R_{k+1,k}^{pc} - R_{k,k+1}^{pe}\right) - \left(R_{k,k-1}^{pc} - R_{k-1,k}^{pe}\right) \tag{13}$$

For the WL state,

$$\frac{\partial w_p}{\partial t} = \frac{I}{qV_aN_{WL}} - \left(R_{w_p,7}^{nc} - R_{7,w_p}^{ne}\right) - R_{w_p}^{sp} \tag{14}$$

where t and z are independent variables, whereas all the other variables, that is, occupation probabilities, are dependent variables of the REM. Details of the REM and also simulation parameters of the investigated QD-SOA can be found in [31]. The rate equations can be solved for a given injected current and input photon density. By solving the rate equations, the longitudinal and temporal variations of the photon density and occupation probabilities can be determined.

3. STATE SPACE MODEL OF QUANTUM-DOT SEMICONDUCTOR OPTICAL AMPLIFIER

The REM of the investigated QD-SOA was presented in the Section 2. As stated before, our objective in this paper is to develop a simple and accurate SSM for QD-SOAs. In order to derive the SSM of the QD-SOA, the dependency of the occupation probabilities on distance must be eliminated. By considering the average values of the occupation probabilities as the REM variables, the carrier density along the cavity obtains a uniform distribution and consequently, z-independent variables will appear in the REM of the QD-SOA. By this assumption and after some manipulations, the SSM of the QD-SOA is derived, where the average values of the occupation probabilities are the state variables of the system.

To find out whether the average values of the occupation probabilities are the appropriate state variables of the SSM, we need to know the effects of uniformity of the occupation probabilities along the cavity on the final results of the REM. Our calculations demonstrate that the variance of the carrier distribution along the cavity does not have a significant impact on the gain dynamics of the amplifier [31]. In other words, the output is weakly dependent on the carrier density variations along the cavity. Consequently, it is reasonable to assume that in the SSM of the QD-SOA, the carrier density distribution along the QD-SOA cavity is completely uniform, that is, we assume that the variance of the carrier density distribution along the cavity is 0. By this assumption, the average values of the occupation probabilities become the state variables of the device [32]. In the following, the details of the mathematical derivation of the SSM are presented.

DOI: 10.1002/jnm

We denote the distance independent occupation probabilities as $\bar{f}_k^p(t), \bar{f}_i^n(t)$, $\bar{w}_n$, and $\bar{w}_p$. These quantities are the average values of occupation probabilities along the cavity and are considered as the state variables of the QD-SOA in the state space. Therefore, the modal gain of QD-SOA in the SSM takes the following form $\bar{g}_{QD}(t)$, which we name it as 'average modal gain' and is given by

$$\bar{g}_{QD} = \sum_{j=0}^{H} g_j\left(\bar{f}_j^n + \bar{f}_j^p - 1\right) \tag{15}$$

Because the state variables do not fluctuate along the QD-SOA cavity, the average modal gain will also be unchanged along the cavity. Depending on the supposed model for QDs, the number of state variables is determined. In our model, InAs QDs have a total of 11 energy levels. Considering the WL states, the dynamics of our investigated QD-SOA can be described by 13 state variables.

As we know from the state space theory, the state update equations of a nonlinear system are generally given by

$$\dot{x}(t) = F_1[x(t), u(t), t] \tag{16a}$$

where $x(t)$ and $u(t)$ denote, respectively, the state and input vectors of the system. Also, the output relation of this system is given by

$$y(t) = F_2[x(t), u(t), t] \tag{16b}$$

where F_1 and F_2 are nonlinear functions of t as well as $x(t)$ and $u(t)$, and where $y(t)$ denotes the output vector. To derive an SSM for QD-SOA, we begin from photon rate equation and obtain a closed-form relation between input and output photon densities. This relation enables us to derive a new relation for stimulated emission rate, and therefore in the next step, we rewrite the rate equations of QD-SOA in the form of state update equations. Derivation details are as follows.

The photon rate equation of the QD-SOA can be rewritten using the state variables as follows:

$$\frac{\partial S}{S} = \left(\bar{g}_{QD} - \alpha\right) \times \partial z \tag{17}$$

By integrating (17), we have

$$\int_{S_{in}}^{S_{out}} \frac{\partial S}{S} = \int_{0}^{L} \left(\bar{g}_{QD} - \alpha\right) \times \partial z \tag{18}$$

Therefore, the relation between the input and output photon densities of QD-SOA becomes

$$S_{out}(t) = S_{in}(t) \exp\left(\left(\bar{g}_{QD} - \alpha\right) \times L\right) \tag{19}$$

where S_{in} and S_{out} are, respectively, the photon densities at the input facet ($z = 0$) and at the output facet ($z = L$) of the QD-SOA, and L is the cavity length. On the other hand, from (17), we have

$$S = \frac{1}{\bar{g}_{QD} - \alpha} \times \frac{\partial S}{\partial z} \tag{20}$$

Substituting (20) in (9), one can obtain

$$R_i^{st}(z,t) = \frac{v_g g_i\left(\bar{f}_i^n + \bar{f}_i^p - 1\right)}{N_Q\left(\bar{g}_{QD} - \alpha\right)} \frac{\partial S(z,t)}{\partial z} \tag{21}$$

Integrating (21) from 0 to L and averaging along the cavity, one can obtain the following expression for stimulated emission rate for the ith energy state as

DOI: 10.1002/jnm

$$\bar{R}_i^{st}(t) = \frac{v_g g_i\left(\bar{f}_i^n + \bar{f}_i^p - 1\right)}{N_Q\left(\bar{g}_{QD} - \alpha\right)}\left[\frac{S(L,t) - S(0,t)}{L}\right] \tag{22}$$

where $S(L,t) = S_{out}(t)$, $S(0,t) = S_{in}(t)$. Substituting (19) in (22), we obtain the relation of stimulated emission rate as

$$\bar{R}_i^{st}(t) = \frac{v_g g_i\left(\bar{f}_i^n + \bar{f}_i^p - 1\right)S_{in}(t)}{N_Q\left(\bar{g}_{QD} - \alpha\right)}\left[\frac{e^{[\bar{g}_{QD}-\alpha]L} - 1}{L}\right] \tag{23}$$

which we name it as 'effective' stimulated emission rate. Also, the effective spontaneous emission is given by

$$\bar{R}_i^{sp}(t) = \frac{\bar{f}_i^n \bar{f}_i^p}{\tau_{iR}}\left(a_{ii}^n + c_{ii}^p \bar{f}_i^p + c_{ii}^n \bar{f}_i^n\right) \tag{24}$$

Similarly, the effective electron capture and escape rates are, respectively, given by

$$\bar{R}_{i+1,i}^{nc}(t) = \frac{\left(1 - \bar{f}_i^n\right)\bar{f}_{i+1}^n}{\tau_{i+1,i}^n}\left(a_{i+1,i}^n + c_{i+1,i}^{np}\bar{w}_p + c_{i+1,i}^{nn}\bar{w}_n\right) \tag{25}$$

$$\bar{R}_{i,i+1}^{ne}(t) = \frac{\left(1 - \bar{f}_{i+1}^n\right)\bar{f}_i^n}{\tau_{i,i+1}^n}\left(a_{i,i+1}^n + c_{i,i+1}^{np}\bar{w}_p + c_{i,i+1}^{nn}\bar{w}_n\right) \tag{26}$$

The effective capture and escape rates for holes in the VB levels are similar to (25) and (26), except that the superscript n is replaced by p. Because the rate equations and consequently the state update equations are not explicit functions of time, QD-SOA is an autonomous system. Hence, the SSM of the device takes the following form

$$\dot{x}(t) = F_1[x(t), u(t)] \tag{27a}$$

$$y(t) = F_2[x(t), u(t)] \tag{27b}$$

where $x = \left[\bar{f}_0^n, \bar{f}_1^n, \bar{f}_2^n, \bar{w}_n, \bar{f}_0^p, \ldots, \bar{f}_7^p, , \bar{w}_p\right]^T$ is the state vector of the system, $u(t) = S_{in}(t)$ is the input variable, $y(t) = S_{out}(t)$ is the output variable, F_1 is the resultant rate of carriers transition rates, and F_2 is the relation of optical gain, that is, (19). Using (23)–(26), we develop the SSM of QD-SOA in the form of (27). The state update equations are given by the following differential equations:

(i) Electron levels.

For the GS,

$$\frac{d\bar{f}_0^n(t)}{dt} = \left(\bar{R}_{1,0}^{nc} - \bar{R}_{0,1}^{ne}\right) - \bar{R}_0^{sp} - \bar{R}_0^{st} \tag{28}$$

For the ith excited state, where $i = 1, 2$,

$$\frac{d\bar{f}_i^n(t)}{dt} = \left(\bar{R}_{i+1,i}^{nc} - \bar{R}_{i,i+1}^{ne}\right) - \left(\bar{R}_{i,i-1}^{nc} - \bar{R}_{i-1,i}^{ne}\right) - \bar{R}_i^{sp} - \bar{R}_i^{st} \tag{29}$$

And for the WL state,

$$\frac{d\bar{w}_n(t)}{dt} = \frac{I}{qV_a N_{WL}} - \left(\bar{R}_{w_n,2}^{nc} - \bar{R}_{2,w_n}^{ne}\right) - \bar{R}_{w_n}^{sp} \tag{30}$$

(ii) Hole levelsFor the GS,

$$\frac{d\bar{f}_0^p(t)}{dt} = \left(\bar{R}_{1,0}^{pc} - \bar{R}_{0,1}^{pe}\right) - \bar{R}_0^{sp} - \bar{R}_0^{st} \tag{31}$$

For the kth excited state, where $k = 1, 2$,

$$\frac{d\bar{f}_k^p(t)}{dt} = \left(\bar{R}_{k+1,k}^{pc} - \bar{R}_{k,k+1}^{pe}\right) - \left(\bar{R}_{k,k-1}^{pc} - \bar{R}_{k-1,k}^{pe}\right) - \bar{R}_k^{sp} - \bar{R}_k^{st} \tag{32}$$

For the kth excited state, where $k > 2$,

DOI: 10.1002/jnm

$$\frac{d\bar{f}_k^p(t)}{dt} = \left(\bar{R}_{k+1,k}^{pc} - \bar{R}_{k,k+1}^{pe}\right) - \left(\bar{R}_{k,k-1}^{pc} - \bar{R}_{k-1,k}^{pe}\right) \tag{33}$$

And for the WL state,

$$\frac{d\bar{w}_p(t)}{dt} = \frac{I}{qV_aN_{WL}} - \left(\bar{R}_{w_p,7}^{nc} - \bar{R}_{7,w_p}^{ne}\right) - \bar{R}_{w_p}^{sp} \tag{34}$$

The output relation of the SSM is described in (19).

4. SIMULATION RESULTS

To investigate the accuracy of the SSM, in this section, we compare the simulation results of the SSM with those of the REM. We use the finite difference method (FDM) to solve the REM and SSM [31]. To solve the REM using FDM, the cavity length is partitioned into M-longitudinal sections (see Figure 3), where the physical quantities in each section are assumed to be constant along the section [31]. To simulate the response of the QD-SOA using the REM and SSM, we need to know the initial state of the system. The initial state (occupation probabilities at $t=0$) can be found by solving the REM and SSM at steady state condition for $S_{\text{in}}=0$. Because at steady state, the time derivatives are zero, the initial state of the system is equivalent to finding the roots of a system of 13 coupled nonlinear algebraic equations, which can be performed by Newton method.

In order to compare the dynamic response of the SSM with that of the REM, the time response of both models are evaluated in condition that a Gaussian-shaped pulse with a width of 0.4 ps and 3 pJ energy is applied at the input facet (see Figure 4(a), (b)). Because the accuracy of the results of the REM depends on the discretization errors, the rate equations of the QD-SOA are solved for different values of Δz. As seen from the Figure, with enhancement the accuracy of numerical calculations, that is, considering smaller values for Δz, the results of the REM become closer to the results obtained by the SSM. Also, Figure 4 (c) illustrates the gain saturation curve of the QD-SOA under different values of Δz. Figure 4(c) demonstrates that the SSM of the QD-SOA not only is accurate in the linear region (low input power) but also is accurate at the nonlinear region (under the gain saturation). For $\Delta z = L/4000$, the results of the REM is very close to the results obtained from the SSM, where the percentage error in calculating the optical gain and output signal is less than 0.5%. These results imply that with lowering the discretization errors, these two models represent even closer results. As is evident, by dividing the cavity length into smaller longitudinal sections, the accuracy of the FDM calculations increases. Because the simulation run time of the REMs are very sensitive to the distance steps in the distance-time grid, considering smaller values for Δz increase the computation time. The required time for solving the REM is much longer than the simulation run time of the SSM.

Furthermore, although the stability of the numerical solving of the state update equations is guaranteed by choosing a small value for Δt, stable solving of the rate equations is dependent on appropriate selection of both Δt and Δz. Therefore, the convergence problems associated with solving the SSM is reduced compared with REMs.

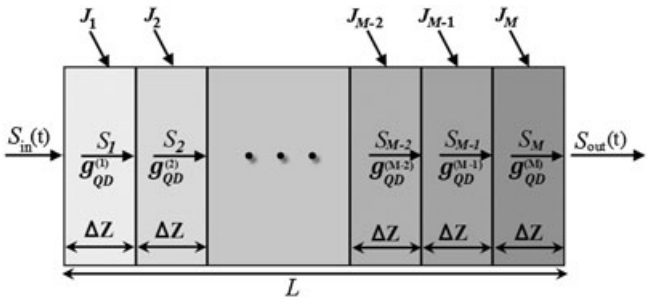

Figure 3. Schematic diagram of the quantum-dot semiconductor optical amplifier cavity which is divided into M identical sections to be used by finite difference method, where L=M.Δz.

DOI: 10.1002/jnm

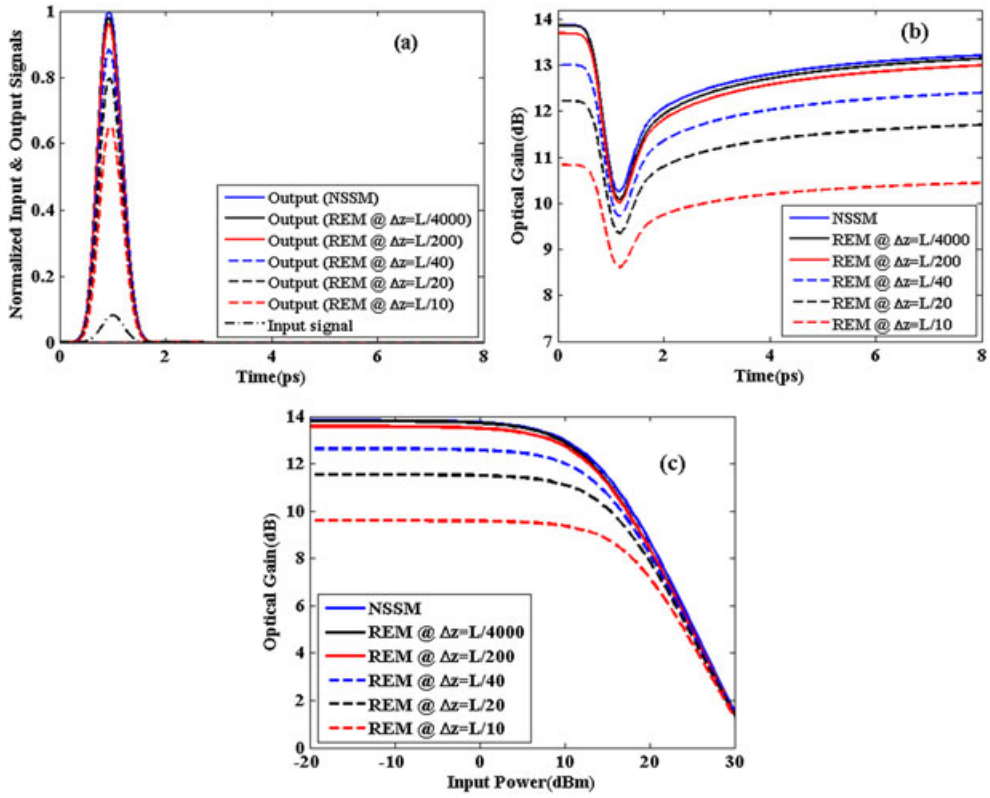

Figure 4. Comparison the results of the state space model with results obtained from solving the rate equations of quantum-dot semiconductor optical amplifier by finite difference method at $\{\Delta z = L/4000, \Delta z = L/200, \Delta z = L/40, \Delta z = L/20, \Delta z = L/10\}$: (a) Gain response, (b) Normalized input and output signals, and (c) gain saturation curves @$J = 4$.

5. CONCLUSION

In this paper, for the first time, we derived an SSM for QD-SOAs. For this purpose, the average values of the occupation probabilities along the QD-SOA cavity were considered as the state variables of the system. Consequently, an SSM for the QD-SOA was derived after some manipulation on the REM. We carried out a comparison between the results of the SSM and REM. Simulation results showed that the SSM of the QD-SOA is accurate in both linear and nonlinear regions. Numerical calculations demonstrated that not only that the SSM is much simpler and faster than the rate equations model but also that the SSM decreases the convergence problems associated with solving QD-SOA rate equations.

REFERENCES

1. Schneider S, Woggon UK, Borri P, Langbein W, Ouyang D, Sellin R, Bimberg D. Ultrafast gain recovery dynamics of the excited state in InGaAs quantum dot amplifiers. *Conference on Lasers and Electro-Optics/Quantum Electronics and Laser Science and Photonic Applications Systems Technologies*, OSA Technical Digest (CD) paper CThH6, 2005.
2. Bakonyi Z, Su H, Onishchukov G, Lester LF, Gray AL, Newell TC, Tuennermann A. High-gain quantum-dot semiconductor optical amplifier for 1300nm. *IEEE J Quantum Electron* 2003; **39**:1409–1413.
3. Schneider S, Borri P, Langbein W, Woggon U, Sellin RL, Ouyang D, Bimberg D. Excited-state gain dynamics in InGaAs quantum-dot amplifiers. *IEEE Photon Technol Lett* 2005; **17**:2014–2016.
4. Kim J, Laemmlin M, Meuer C, Bimberg D, Eisenstein G. Theoretical and experimental study of high-speed small signal cross-gain modulation of quantum-dot semiconductor optical amplifiers. *IEEE J Quantum Electron* 2009; **45**:240–248.
5. Yi Y, Lirong H, Meng X, Peng T, Dexiu H. Enhancement of gain recovery rate and cross-gain modulation bandwidth using a two-electrode quantum-dot semiconductor optical amplifier. *J Opt Soc Am B* 2010; **27**:2211–2217.
6. Berg TW, Bischoff S, Magnusdottir I, Moerk J. Ultrafast gain recovery and modulation limitations in self-assembled quantum-dot devices. *IEEE Photon Technol Lett* 2001; **13**:541–543.
7. Meuer C, Kim J, Laemmlin M, Liebich S, Capua A, Eisenstein G, Kovsh AR, Mikhrin SS, Krestnikov IL, Bimberg D. Static gain saturation in quantum dot semiconductor optical amplifiers. *Opt Express* 2008; **16**:8269–8279.
8. Vallaitis T, Koos C, Bonk R, Freude W, Laemmlin M, Meuer C, Bimberg D, Leuthold J. Slow and fast dynamics of gain and phase in a quantum dot semiconductor optical amplifier. *Opt Express* 2008; **16**:170–178.

DOI: 10.1002/jnm

9. Sugawara M, Hatori N, Ishida M, Ebe H, Arakawa Y, Akiyama T, Otsubo T, Yamamoto Y, Nakata Y. Recent progress in self-assembled quantum-dot optical devices for optical telecommunication: temperature-insensitive 10 Gb s-1 directly modulated lasers and 40 Gb s-1 signal-regenerative amplifiers. *J Phys D: Appl Phys* 2005; **38**:2126–2134.
10. Schmidt-Langhorst C, Meuer C, Ludwig R, Puris D, Bonk R, Vallaitis T, Bimberg D, Petermann K, Leuthold J, Schubert C. Quantum-dot semiconductor optical booster amplifier with ultrafast gain recovery for pattern-effect free amplification of 80 Gb/s RZ-OOK date signals *Proc. ECOC, Vienna, Austria*, Paper 6.2.1, 2009.
11. Contestabile G, Maruta A, Sekiguchi S, Morito K, Sugawara M, Kitayama K. 160 Gb/s cross gain modulation in quantum dot SOA at 1550 nm. *Proc. ECOC 2009*; *Vienna, Austria*, Paper PDP 1.4.
12. Rostami A, Nejad HBA, Qartavol RM, Saghai HR. Tb/s optical logic gates based on quantum-dot semiconductor optical amplifiers. *IEEE J Quantum Electron* 2010; **46**:354–360.
13. Sugawara M, Hatori N, Akiyama T, Nakata Y, Ishikawa H. Quantum-dot semiconductor optical amplifiers for high bit-rate signal processing over 40 Gbit/s. *Jpn J Appl Phys* 2001; **40**:L488–L491.
14. Sugawara M, Akiyama T, Hatori N, Nakata Y, Ebe H, Ishikawa H. Quantum-dot semiconductor optical amplifiers for high-bit-rate signal processing up to 160Gb $s-1$ and a new scheme of 3R regenerators. *Meas Sci Technol* 2002; **13**:1683–1691.
15. Xiao JL, Huang YZ. Numerical analysis of gain saturation, noise figure, and carrier distribution for quantum-dot semiconductor-optical amplifiers. *IEEE J Quantum Electron* 2008; **44**:448–455.
16. Chow WW, Koch SW. Semiconductor-Laser Fundamentals: Physics of the Gain Materials. Springer-Verlag: Berlin, 1999.
17. van der Poel M, Gehrig E, Hess O, Birkedal D, Hvam JM. Ultrafast gain dynamics in quantum-dot amplifiers: theoretical analysis and experimental investigations. *IEEE J Quantum Electron* 2005; **41**:1115–1123.
18. Gehrig E, Hess O. Mesoscopic spatiotemporal theory for quantum-dot lasers. *Phys Rev A* 2002; **65**:033804.
19. Chow WW, Koch SW. Theory of semiconductor quantum-dot laser dynamics. *IEEE J Quantum Electron* 2005; **41**:495–505.
20. Reschner DW, Gehrig E, Hess O. Pulse amplification and spatio-spectral hole-burning in inhomogeneously broadened quantum-dot semiconductor optical amplifiers. *IEEE J Quantum Electron* 2009; **45**:21–33.
21. Meuer C, Kim J, Laemmlin M, Liebich S, Eisenstein G, Bonk R, Vallaitis T, Leuthold J, Kovsh A, Krestnikov I, Bimberg D. High-speed small-signal cross-gain modulation in quantum-dot semiconductor optical amplifiers at 1.3 μm. *IEEE J Sel Topics Quantum Electron* 2009; **15**:749–756.
22. Sugawara M, Ebe H, Hatori N, Ishida M, Arakawa Y, Akiyama T, Otsubo K, Nakata Y. Theory of optical signal amplification and processing by quantum-dot semiconductor optical amplifiers. *Phys Rev B* 2004; **69**:235332.
23. Bilenca A, Eisenstein G. On the noise properties of linear and nonlinear quantum-dot semiconductor optical amplifiers: The impact of inhomogeneously broadened gain and fast carrier dynamics. *IEEE J Quantum Electron* 2004; **40**: 690–702.
24. Qasaimeh O. Characteristics of cross-gain (XG) wavelength conversion in quantum dot semiconductor optical amplifiers. *IEEE Photon Technol Lett* 2004; **16**:542–544.
25. Kim J, Chuang SL. Small-signal cross-gain modulation of quantum-dot semiconductor optical amplifiers. *IEEE Photon Technol Lett* 2006; **18**:2538–2540.
26. Uskov AV, Berg TW, Mork J. Theory of pulse-train amplification without patterning effects in quantum-dot semiconductor optical amplifiers. *IEEE J Quantum Electron* 2004; **40**:306–320.
27. Ababneh JI, Qasaimeh O. Simple model for quantum-dot semiconductor optical amplifiers using artificial neural networks. *IEEE Electron Device Lett* 2006; **53**:1543–1550.
28. Qasaimeh O. Effect of doping on the optical characteristics of quantum dot semiconductor optical amplifiers. *J Lightw Technol* 2009; **27**:1978–1984.
29. Qasaimeh O. Ultra-fast gain recovery and compression due to Auger-assisted relaxation in quantum dot semiconductor optical amplifiers. *J Lightw Technol* 2009; **27**:2530–2536.
30. Fiore A, Markus A. Differential gain and gain compression in quantum dot lasers. *IEEE J Quantum Electron* 2007; **43**:287–294.
31. Taleb H, Abedi K, Golmohammadi S. Operation of quantum-dot semiconductor optical amplifiers under nonuniform current injection. *Appl Opt* 2011; **50**:608–617.
32. Kuntze SB, Zilkie AJ, Pavel L, Aitchison JS. Nonlinear state-space model of semiconductor optical amplifiers with gain compression for system design and analysis. *J Lightw Technol* 2008; **26**: 2274–2281.

AUTHOR'S BIOGRAPHIES

Hussein Taleb was born in Najafabad, Isfahan, Iran, in 1985. He received his BS in Electrical Engineering from Islamic Azad University, Najafabad branch, Iran in 2008. He received his MS degree (with highest honors) in Optoelectronics Engineering from the Islamic Azad University, Ahar Branch, Iran in 2010. He is currently working toward his PhD degree on the topic of numerical simulation of quantum dot-based optoelectronic devices at Shahid Beheshti University, Tehran, Iran.

DOI: 10.1002/jnm

Kambiz Abedi was born in Ahar, Iran, in 1970. He received his BS degree from University of Tehran, Iran, in 1992, his MS degree from Iran University of Science and Technology, Tehran, Iran in 1995, and his PhD degree from Tarbiat Modares University, Tehran, Iran, in 2008, all in Electrical Engineering. His research interests include design, circuit modeling, and numerical simulation of optoelectronic devices, semiconductor lasers, optical modulators, optical amplifiers and detectors.

Dr. Abedi is currently an assistant professor at Shahid Beheshti University, Tehran, Iran.

Saeed Golmohammadi was born in Heris, Tabriz, Iran, in 1976. He received his B.S., M.S., and Ph.D. in electrical engineering from the University of Tabriz in Iran in 1998, Shiraz University in Iran in 2001, and Tarbiat Modares University in Iran in 2008, respectively. He is now an assistant professor in the nanophotonics group, Department of Engineering and Emerging Technologies, at the University of Tabriz, Tabriz, Iran. His fields of interests are fiber-optic devices, optical communication systems, and optical networking.

DOI: 10.1002/jnm